



ELSEVIER

Deep-Sea Research II 52 (2005) 853–873

DEEP-SEA RESEARCH
PART II

www.elsevier.com/locate/dsr2

Modelling the generation of Haida Eddies

E. Di Lorenzo^{a,*}, M.G.G. Foreman^b, W.R. Crawford^b

^a*School of Earth and Atmospheric Sciences, Georgia Institute of Technology, 311 Ferst Drive, Atlanta, GA 30306, USA*

^b*Institute of Ocean Sciences, Fisheries and Oceans Canada, Sidney, BC, Canada*

Accepted 5 February 2005

Available online 7 April 2005

Abstract

A numerical model forced with average annual cycles of climatological winds, surface heat flux, and temperature and salinity along the open boundaries is used to demonstrate that Haida Eddies are typically generated each winter off Cape St. James, at the southern tip of the Queen Charlotte Islands of western Canada. Annual cycles of sea-surface elevation measured at coastal tide gauges and TOPEX/POSEIDON crossover locations are reproduced with reasonable accuracy. Model sensitivity studies show that Haida Eddies are baroclinic in nature and are generated by the merging of several smaller eddies that have been formed to the west of Cape St. James. The generation mechanism does not require the existence of instability processes and is associated with the mean advection of warmer and fresher water masses around the cape from Hecate Strait and from the southeast. These advected water masses generate plumes of buoyant flow, which intensify and sustain small patches of anticyclonic circulation immediately to the northwest of the cape. When the flow is stronger, several of these smaller eddies can merge to generate a larger eddy, the Haida Eddy. Similar to observations, a typical generation-shedding cycle for larger Haida Eddies in the model is 3–4 months. Consistent with previous in situ water property measurements, these experiments show that the eddies are generally comprised of mixed-layer water from Hecate Strait, Queen Charlotte Sound, and the continental shelves off northern Vancouver Island. Their vertical extent during the mature stage is roughly 1000 m.

© 2005 Elsevier Ltd. All rights reserved.

1. Introduction

A recent study (Crawford et al., 2002) suggests that Haida Eddies are generated off Cape St. James at the southern tip of the Queen Charlotte Islands, British Columbia (Fig. 1) when pressure-driven outflows from Hecate Strait encounter a

narrow continental shelf and steep bathymetry. Though these eddies are formed every winter, the precise number generated and their particular size seem to vary with the wind and both near- and far-field alongshore flow conditions. Once they advect into the Gulf of Alaska, the eddies are characterized by anticyclonic rotation, a baroclinic structure extending in depth to at least 1000 m, a diameter of 150–300 km, a sea-surface height anomaly (SSHA) of up to 40 cm, and waters that are typically less

*Corresponding author. Tel.: +1 404 894 3994.

E-mail address: edl@eas.gatech.edu (E. Di Lorenzo).

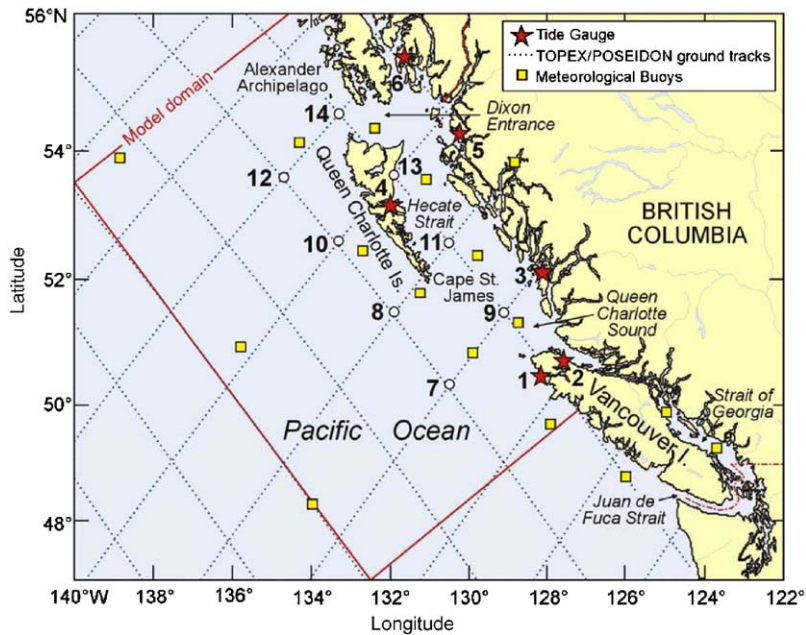


Fig. 1. Region of study showing the model domain, Environment Canada and Department of Fisheries and Oceans weather buoys, and tide gauges (numbered 1–6) and TP crossover sites (numbered 7–14) used to evaluate model accuracy.

saline and warmer (below the top 100 m) than the surrounding ocean (Crawford, 2002).

The particularly large eddies that were formed during the 1997–98 El Niño were initially identified in sea-surface height (SSH) images produced by the Colorado Center for Astro-dynamics Research (http://e450.colorado.edu/realtime/gsfc_global-real-time_ssh/). Crawford et al. (2002) present (in their Fig. 4) their own analysis of a series of 10-day TOPEX/POSEIDON (TP) and ERS-2 altimetry snapshots showing Haida Eddy development between November 1997 and February 1998. Whitney and Robert (2002) and Mackas and Galbraith (2002) provide overviews of the nutrient and zooplankton characteristics of Haida Eddies. In particular, in situ sampling of the 1998 eddies and their counterparts in more recent years have revealed water properties and larvae that are typical of winter coastal water normally found in Queen Charlotte Sound and Hecate Strait (Batten and Crawford, 2005). As a result, these eddies are thought to play a significant role in the regional ecosystem as they sweep plankton, larvae, and nutrients offshore, thereby reducing the biological

productivity on the shelf and increasing the offshore productivity as the eddy decays and releases its contents to the ambient ocean (Crawford, 2003; Johnson et al., 2005; Whitney and Robert, 2002).

Two previous numerical studies have addressed the generation of eddies in the Gulf of Alaska. Analysing results from a $1/8^\circ$, six-layer, isopycnal model (Hurlburt et al., 1996) simulation of the North Pacific for 1981–94, Melsom et al. (1999) described the generation of large eddies off Baranoff Island and the Queen Charlotte Islands at the end of the 1982–83 El Niño. Eddies off Baranoff Island are commonly referred to as Sitka Eddies and were first studied by Tabata (1982), while the Queen Charlotte eddies have come to be known as Haida Eddies, in reference to Haida Gwaii, the native name for the Queen Charlotte Islands. Through correlations between pseudo (e.g., from an atmospheric model) wind stress and sea levels measured at the Sitka tide gauge, Melsom et al. (1999) suggested that the 1983 eddies arose predominantly from baroclinic instabilities associated with ENSO teleconnections

(Kelvin waves) rather than local wind forcing. However, in other years such as 1992, local atmospheric forcing was thought to play a larger role in eddy generation. This study was extended by Murray et al. (2001) using simulations from the same six-layered model but a more refined $1/16^\circ$ grid. In this case, the main conclusion was that the formation of a coast-wide train of large anticyclonic eddies similar to those described by Thomson and Gower (1998) was caused by baroclinic instabilities associated with the arrival of Kelvin waves at the peak of the annual cycle in the Alaska Current.

Although both the Melsom et al. (1999) and Murray et al. (2001) model simulations claimed to have their coastlines defined at the 200 m isobath, Fig. 6 and plate 1 in those respective papers indicate that a more restrictive definition was used along the continental shelf between Vancouver Island and the Queen Charlotte Islands. Despite the fact that Hecate Strait and Queen Charlotte Sound have depths greater than 400 m, both regions seem to be missing from the two model domains. Therefore, in light of the Whitney and Robert (2002) conclusion on the origin of water in Haida Eddies, a re-examination of the eddy generation dynamics described by Melsom et al. (1999) and Murray et al. (2001) would seem to be warranted using a model that includes all the continental shelf.

Crawford et al. (2002) (henceforth CCFG02) argue that although eddies generated to the north of Cape St. James may arise from the instabilities described by Melsom et al. (1999) and Murray et al. (2001), it is unlikely that these two models accurately simulate details of the flow near Cape St. James and hence Haida Eddy formation. To substantiate this conclusion, CCFG02 cite the laboratory studies of Cenedese and Whitehead (2000) (henceforth CW00), the existence of a tidal residual eddy west of the cape (Thomson and Wilson, 1987), and current meter observations that show strong southward components in the residual flows both to the east and west of the cape. In particular, persistent southward flows observed to the west of the cape would not be consistent with conditions required for baroclinic instability. Two AVHRR figures in Thomson and Wilson (1987)

also show clear anticyclonic eddies west and southwest of Cape St. James. The CCFG02 hypothesis is that strong northwestward winds result in large outflows past the cape, and eddies being formed through mechanisms similar to those described in the CW00 rotating tank experiments. In particular, applying parameter values characteristic of this region, CCFG02 determine that eddies should hug the shore when their radius is about 40 km or less, and detach when bigger. This size limit is consistent with both the tidal residual eddies observed and modelled by Thomson and Wilson (1987) and the early Haida 1998 altimeter images.

Nof et al. (2002) recently described an eddy formation mechanism similar to that of CW00. Motivated by the “teddies” generated when Indonesian Throughflow empties into the Indian Ocean northwest of Australia, they show that on a β -plane, eddies detach periodically from an inflow source when their size is sufficiently large that the westward drift exceeds the growth rate.

The objective of this study is to carry out numerical experiments to determine the generation mechanism of Haida Eddies. In particular, we wish to confirm or refute the applicability of the mechanisms suggested by CW00, Nof et al. (2002), Melsom et al. (1999) and Murray et al. (2001).

2. Model and forcing details

The model used in our studies was the Regional Ocean Modeling System (ROMS), a descendant of SCRUM (Song and Haidvogel, 1994) that is garnering wide usage (Di Lorenzo, 2003; Haidvogel et al., 2000; Marchesiello et al., 2001a; She and Klinck, 2000). The model uses a generalized sigma-coordinate system in the vertical and a curvilinear horizontal grid. The model domain chosen for our application extends from northern Vancouver Island to the Alexander Archipelago of southeast Alaska (Fig. 1) and has an approximate offshore extent of 650 km. There are 20 levels in the vertical with enhanced resolution in the surface and bottom boundary layers and a horizontal resolution of approximately 8 km. Bathymetry was

obtained by a smooth interpolation of data from a variety of sources including ETOP05 and Smith and Sandwell (1997) for values off the continental shelves, and National Oceanic and Atmospheric Administration (NOAA) and Canadian Hydrographic Service charts and databases for depths along the British Columbia and Alaskan shelves and inland waters. The minimum model depth is 7 m in the coastal region, and the maximum is 3800 m in the offshore. A no-slip lateral boundary condition is used for all simulations except one sensitivity study, which was carried out with a free-slip condition.

Relevant to the generation and maintenance of eddies, ROMS provides several options for computing the advective terms in the momentum equations. Although most of our numerical simulations employed a third-order upstream bias scheme, a less accurate second-order centred scheme was used once to emphasize the importance of a more accurate representation of advection.

A modified radiation condition (Marchesiello et al., 2001b) coupled with nudging to climatology is used along the three open boundaries to ensure a stable, long-term integration of the model. The nudging is stronger (timescale of 1 day) for inward flow and weaker (timescale of 1 year) for outward. More complete descriptions of the model numerics, open-boundary conditions, and mixed-layer parameterizations can be found in Shchepetkin and McWilliams (1998, 2003) and Large et al. (1994). Initial and open-boundary conditions for the model are taken from the Levitus et al. (1994) temperature and salinity monthly climatologies.

Two different sources for wind forcing were evaluated. The first is the NCEP Pacific Ocean re-analysis monthly mean (1980-present) wind stresses at a resolution of 1 by 1.5°. The second is an empirical–statistical re-analysis (Faucher et al., 1999) of winds measured at 13 buoys (jointly maintained by Environment Canada and the Department of Fisheries and Oceans) off the British Columbia coast (Fig. 1). Faucher et al. (1999) not only claim that their winds are more accurate than the NCEP re-analysed values interpolated to the buoy locations, but they also claim

these winds recover more than 60% of the observed wind variance during an independent verification period. Fig. 2 shows the two sets of bi-monthly mean wind stress values. There is reasonable agreement for the three sites furthest offshore though the NCEP magnitudes are generally larger, perhaps reflecting differences in the averaging procedure and/or in the height of the anemometers (Cherniawsky and Crawford, 1996). At the inshore locations, the NCEP winds are extrapolated from the offshore location using an objective analysis procedure (Bretherton et al., 1976) and miss the seasonal changes in direction that characterize the buoy winds. Although these differences in the winds are likely to be important in the seasonal changes of the coastal dynamics, the model experiments suggest that they are not crucial to the generation of Haida Eddies. We will therefore use the NCEP winds alone for the model experiments. The winds are mapped to the model grid using objective analysis with a horizontal decorrelation length scale of 200 km.

3. Annual cycle simulations

The first model objective is to simulate the annual cycle. This was accomplished by running the model for a period of 12 years with forcing from repeated annual cycles of climatological winds, boundary temperatures and salinities, and NCEP surface heat fluxes. In addition to these forcing functions, the surface fluxes are also corrected using a nudging to the Levitus et al. (1994) climatological SST. Fig. 3 shows average monthly sea-surface elevation from the last 10 years of the integration. Consistent with north-westward winds, November–February are characterized by positive elevations along the coast and in Hecate Strait. Anticyclonic circulation patterns with higher SSHs in their centres appear as lighter regions in Fig. 3. Sea level rises along the mainland coast with the beginning of storm winds in mid-October. By November this rise has increased and extended westward to the Queen Charlotte Islands. The beginning of the Haida Eddy formation is clearly seen to the west of Cape St. James in the December mean. In January and February, the

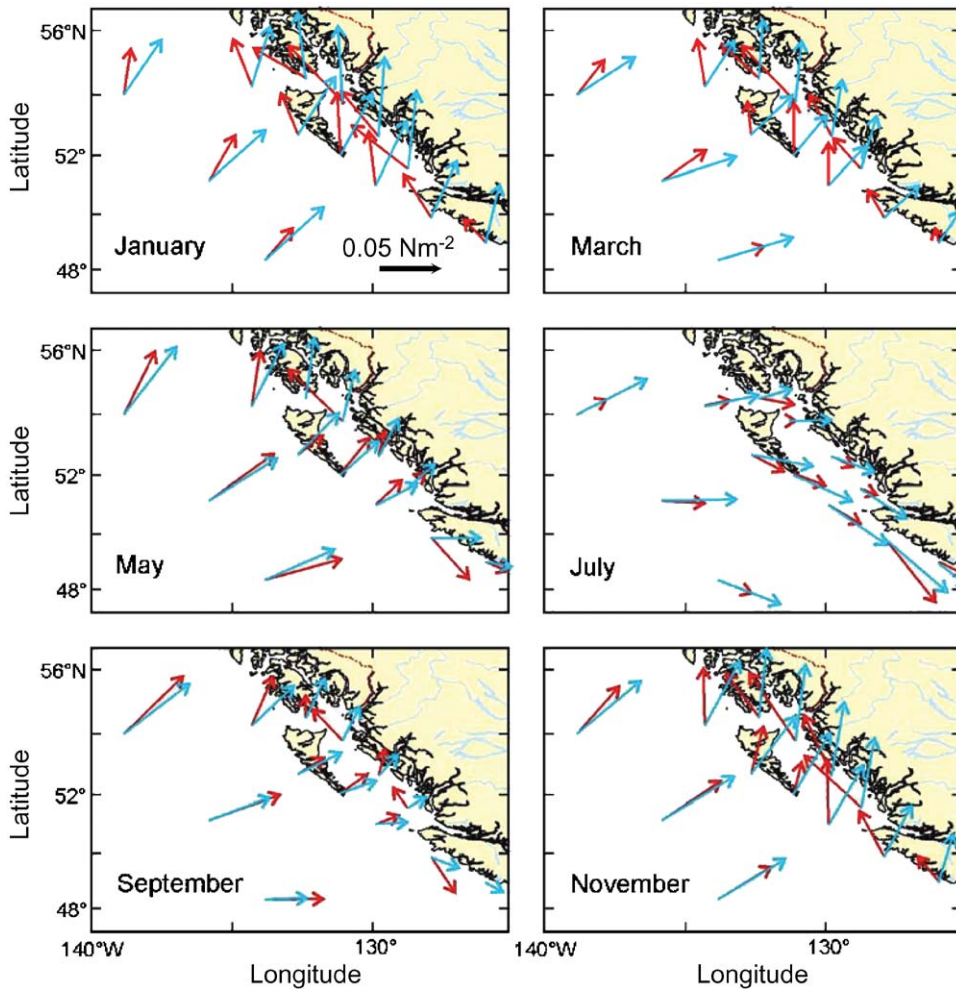


Fig. 2. Bi-monthly mean wind stress at offshore buoy locations from interpolated NCEP 40-year re-analysis project (blue) values, and the Faucher et al. (1999) CANFIS reconstruction (red).

anomalous positive height associated with the formation of the Haida Eddy intensifies. By March, the eddy has become a fully developed coherent structure and is detached from the coast. An animation of the full 12-year simulation (<http://www-sci.pac.dfo-mpo.gc.ca/dsr2/>) reveals interannual variability in migration paths after detachment and this is evident in the mean by smeared higher offshore elevations throughout the spring and summer panels of Fig. 3.

By September, interactions with the model boundaries have effectively destroyed the eddies and produced higher elevations along the western,

and to a lesser extent the southern, boundary. The 12-year animation also shows irregular eddy formation throughout the winter months, and from year to year. This formation seems to depend on the magnitude of the SSH gradients around Cape St. James, which in turn dictate the strength of the southward flows past the east side of the cape. There is considerable interannual variability with on average, 1.3 eddies being formed each winter. More details on the formation mechanism will follow in Section 4.

In the summer months, southeastward winds are seen to produce negative SSHAs (relative to the

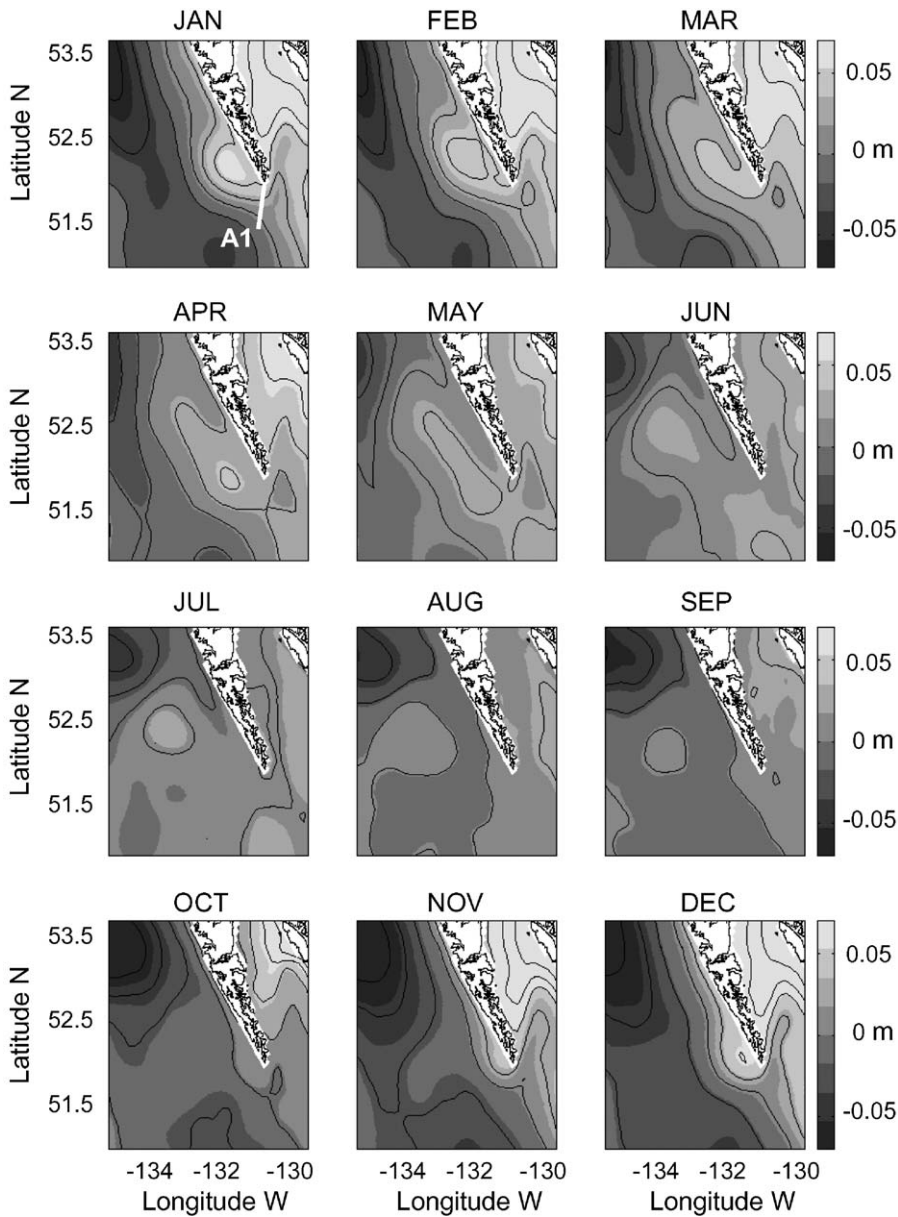


Fig. 3. Average monthly model SSH (m) from a 12-year simulation with climatological forcing. Location of transect A1 is showed in the upper left panel.

annual mean) along the coast and in Hecate Strait (Fig. 3). By October these anomalies have moved offshore and deepen to their largest values in November as the northwestward winter winds begin to rise. The annual pattern in SSHA is consistent with that calculated from TP altimetry

and shown in Fig. 3 of Foreman et al. (1998). In the winter, there are positive anomalies along the shelf regions and negative anomalies offshore while in the summer, that pattern reverses. Fig. 4 quantifies the magnitude and timing the annual cycle. Twelve-year time series of SSHA are shown

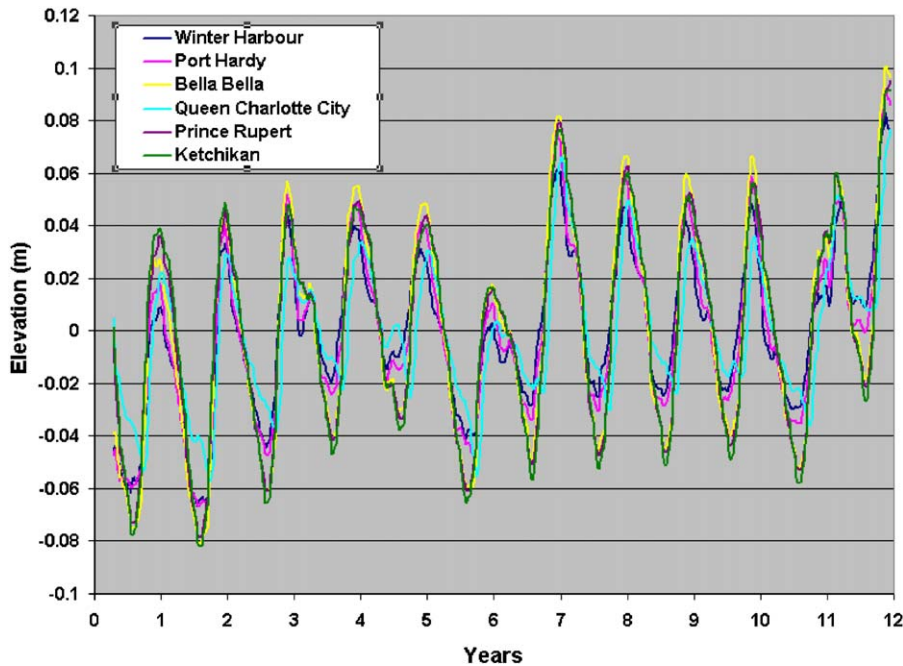


Fig. 4. Sea-surface elevations at model cells nearest the tide gauge locations shown in Fig. 1. (See Table 1 for numbering.) Forcing was comprised of climatological monthly winds, boundary temperatures and salinities, and surface fluxes. The time series begin in April.

for the model grid cells nearest to the six tide gauge locations shown in Fig. 1. All sites display seasonal patterns that vary slightly in magnitude but are basically in phase. However, interannual variability is evident even though the annual forcing is identical each year. This suggests a high degree of non-linearity in the dynamics. Table 1 lists the amplitudes and phase lags of the annual cycle that is computed through least-squares fits over the last 8 years. Analogous values computed from tide gauge observations over the period 1992–99 and TP altimetry over the period 1993–00 are shown for comparison. Because the model does not include tides or atmospheric pressure, the tide gauge values were low-pass filtered to remove the tides and corrected for inverse barometer effects using the Koblinsky et al. (1999) relationship and pressures measured at the closest meteorological buoys shown in Fig. 1. The altimetry was processed similarly, using the same inverse barometer correction and tide removal (through the harmonic analysis) described in Cherniawsky et al. (2001).

The model amplitudes are consistently smaller than the tide gauge values. This could be for a variety of reasons including: (i) a coarse-model resolution that not only provides insufficient representation of the bathymetry and coastline but also means that the model tide gauge locations are not sufficiently close to the true locations; (ii) inaccurate ocean-boundary forcing (due to their 1° resolution, the Levitus et al. (1994) temperatures and salinities may be overly smoothed, particularly along the continental shelves); (iii) average NCEP monthly winds that have smoothed out the shorter period storms that produce extreme elevations and, as seen in Fig. 2, have seasonal direction errors; (iv) inaccurate surface-boundary forcing; (v) missing freshwater input from strong coastal runoff in winter. In particular, we suspect that an under-representation of the alongshore component of the winter winds (reason (iii)) near the coast is the largest factor behind this amplitude discrepancy. However, the model phases are reasonably accurate with the maximum discrepancies occurring at

Table 1
Comparison of observed and model annual signals

Station name	Number in Fig. 1	Observed amplitude	Observed phase	Model amplitude	Model phase
Winter Harbour	1	11.9	12.6	2.5	−19.7
Port Hardy	2	8.2	18.3	3.3	−15.7
Bella Bella	3	9.3	8.4	4.5	−7.8
QC City	4	3.0	4.5	2.5	18.9
Prince Rupert	5	8.1	10.2	4.4	−1.3
Ketchikan	6	7.2	−4.7	4.5	−0.7
TP crossover	7	7.0	237.8	1.6	157.1
TP crossover	8	4.4	208.4	2.0	137.0
TP crossover	9	5.3	24.1	2.8	14.0
TP crossover	10	3.2	221.7	2.2	116.6
TP crossover	11	3.0	−10.0	1.1	57.0
TP crossover	12	4.6	225.1	2.5	114.2
TP crossover	13	3.7	−42.3	2.5	17.3
TP crossover	14	6.3	−0.2	3.2	14.0

Note: Amplitudes (cm) are with respect to mean sea level and phase lags (degrees) are with respect to 000 PST January 1.

Winter Harbour and Port Hardy where the model timing is about a month (30°) early.

Slightly poorer agreement is found between model amplitudes and those at the TP crossover locations. Whereas the amplitude and phase differences at shelf sites (9, 11, 13, 14) and the amplitude differences at offshore sites (7, 8, 10, 12) are comparable to those for the tide gauges, the offshore model phases are too early by $70\text{--}110^\circ$. These phase shifts of approximately 2–4 months probably arise from a combination of inaccuracies in the forcing (as described above) and boundary conditions that have not allowed eddies (and other features) to completely leave the model domain (see <http://www-sci.pac.dfo-mpo.gc.ca/dsr2/>). This may be because the open/radiating boundaries are forced using very smooth data with actual resolution much coarser than the Levitus et al. (1994) 1° values, rather than output from larger scale models. However, our model has generally captured the dramatic difference in phases among the TP locations. The on-shelf sites (9, 11, 13, 14) have highs in the winter (consistent with the tide gauge timing) while the offshore sites (7, 8, 10, 12) have their highs in late summer (223° would be mid-August). These values are consistent with the more detailed spatial patterns shown in Fig. 3 of Foreman et al. (1998).

4. The eddy generation mechanism

In Section 3, we showed that despite some inaccuracies in the magnitude and timing of the annual cycle, the model is capable of simulating eddy generation off Cape St. James during winter. In order to simplify and better understand the processes involved in the generation mechanism, an experiment was carried out with constant climatological winter winds and surface heat flux. The initial and boundary conditions for temperature and salinity were set to the climatological value for the month of January. The model results (experiment RUN_JAN in Table 2) show the generation and shedding of numerous eddies off Cape St. James during a 10-year simulation. Animations for all the experiments discussed in this section can be found at <http://www-sci.pac.dfo-mpo.gc.ca/dsr2/>. Smaller eddies with radii of up to approximately 40 km are seen to be generated almost continuously from the cape, although stronger eddies (radii larger than 40 km) are not generated at regular intervals.

During times of stronger cross-shelf gradients in the SSHA to the west and southwest of the cape, eddies are generated more vigorously and are seen to merge into a larger Haida Eddy (radii up to 100 km) located slightly to the northwest. Even-

Table 2
Experiment configuration for the constant winter forcing simulations

Experiment name	Coriolis	Topography	TS boundary conditions	Horizontal advection scheme
RUN_JAN	β -plane	$h = H(x, y)$	JAN clim.	3rd ord. UP
RUN_JAN_NO_BETA	f -plane	$h = H(x, y)$	JAN clim.	3rd ord. UP
RUN_JAN_FLAT_H	β -plane	$h = 500$ m	JAN clim.	3rd ord. UP
RUN_JAN_FLAT_H_BOUND $h = 500$ m + boundary	β -plane	3rd ord. UP	JAN clim.	
RUN_JAN_FLAT_H_BOUND 3X $h = 500$ m + boundary	β -plane	3rd ord. UP	JAN clim.	
RUN_JAN_FLAT_H_BOUND FREE_SLIP	β -plane	3rd ord. UP	JAN clim.	
$h = 500$ m + boundary	JAN clim.	3rd ord. UP		
RUN_JAN_NO_BAR	β -plane	$h = H(x, y)$	Constant	3rd ord. UP
RUN_JAN_ADV2	β -plane	$h = H(x, y)$	JAN clim.	2rd ord. CEN

tually, this Haida Eddy increases in size and intensity, and detaches from the shelf region moving, on average, in a west-northwesterly direction.

The time sequences of SSH anomalies and SST for one of the larger eddies is shown in Figs. 5 and 6. The time between successive snapshots is 5 days. Several small patches of positive SSHA (anticyclonic circulation) are seen to be created at the cape, move to the northwest, and then merge into a bigger eddy that lies further offshore. Because of the cross-shore gradients in temperature and salinity, these patches contain more buoyant fluid as a result of the advection of warmer fresher water from Hecate Strait into colder saltier offshore waters. The difference in density between the core of these patches and the ambient water intensifies and sustains the anticyclonic circulation of these patches as smaller independent eddies. Five successive occurrences of these patches initially appear in the panels at the 5-day intervals labelled 200, 205, 211, 216 and 222, respectively. Each is a distinct small eddy. The first patch becomes the beginning of a Haida Eddy that intensifies as the next three patches successively merge with it. However, the fifth patch does not quite merge because at the time when it starts to do so, the main eddy has moved too far westward. Instead this fifth patch is left behind to become the beginning of what could be the next Haida Eddy.

As the first Haida Eddy moves towards the offshore region it affects the mean regional circulation patterns by decreasing cross-shelf elevation gradients. This reduces the speed of the southward currents along the eastern side of Cape St. James and the advection of warmer more buoyant flow off the cape into the offshore waters. As a result, the generation of stronger eddies is inhibited. In fact, the next strong eddy does not form off the cape for another 80 days, although smaller eddies continue to generate following the same process. The interaction between the Haida Eddies and the strength of the mean flow is the likely reason that strong eddies are not generated at a regular interval.

These RUN_JAN model results suggest that the strength of the southward currents and the consequent advection of more buoyant flow around Cape St. James are necessary conditions for the strong eddy formation. To further verify this hypothesis we plot a time series of the mean velocity across transect A1 (see Fig. 3) vertically averaged over the top 100 m of the ocean, and use it as an index for both the strength of the currents and the offshore advection of warmer waters. This time series (Fig. 7) shows three strong maxima that correspond to the generation of the three strongest Haida Eddies observed in the entire model simulation (see SSH animation at <http://www-sci.pac.dfo-mpo.gc.ca/dsr2/>). Based on this result

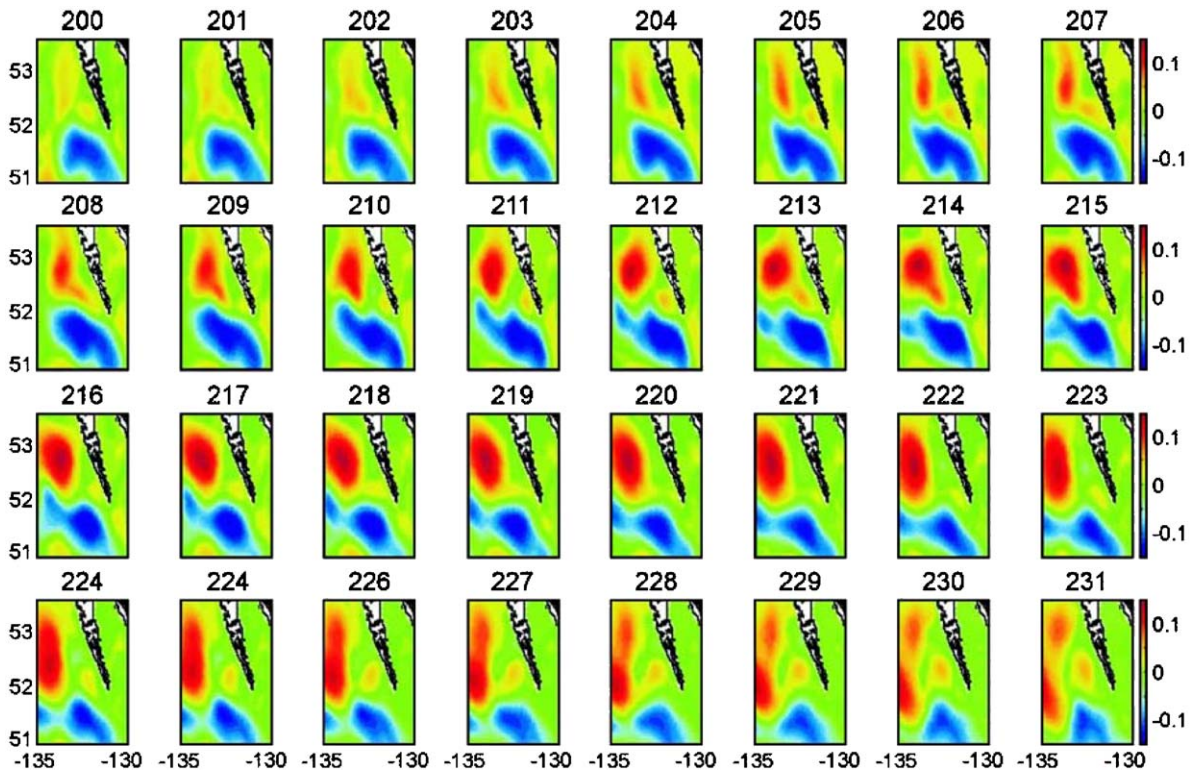


Fig. 5. Time sequences (5-day interval) of model SSH anomalies (m) arising from constant January winds and surface heat fluxes (experiment RUN_JAN).

we construct a composite of the generation sequence by averaging all the snapshots of SST and SSHA for which the average current speed across transect A1 exceeds 15 cm s^{-1} (the points above horizontal black line in Fig. 7). We refer to this composite as ‘day 0’ in the maps shown in Fig. 8. We then perform the same composite averaging to capture the SST and SSH patterns 40 days prior to ‘day 0’ and 40 and 80 days after ‘day 0’ (the remaining maps in Fig. 8). In the SST sequence at day -40 we find that the Queen Charlotte Islands act as a barrier between the warm waters in Hecate Strait and the colder waters offshore. At the southern tip of the island (Cape St. James) these two water masses come in contact and the offshore advection is visible as a plume of warmer water. The horizontal density gradient between this pool of buoyant flow and the denser ambient waters west of the cape intensifies and sustains anticyclonic circulation. As we progress forward in the

sequence the spreading of warmer SST to the northwest is associated with the path of the smaller eddies that originate at the cape and merge into a larger eddy offshore (as evident in Figs. 5 and 6 and the SSH animation). As a result the cross-shore gradient in temperature decreases at the end of the generation sequence. The sequence of SSHs simultaneous with the SSTs shows the intensification of positive anomalies around and to the northwest of the cape as we progress forward in time. At day 40 the positive anomalies have spread further to the northwest and at day 80 the signature of a more developed eddy is apparent. The signature of the generation and migration of the eddies is also evident in the long-term model SSH mean (Fig. 10A, experiment RUN_JAN).

This generation process is consistent with the CW00 lab experiment where a flux of buoyant fluid flowing around the cape was found to generate baroclinic anticyclonic vortices that are

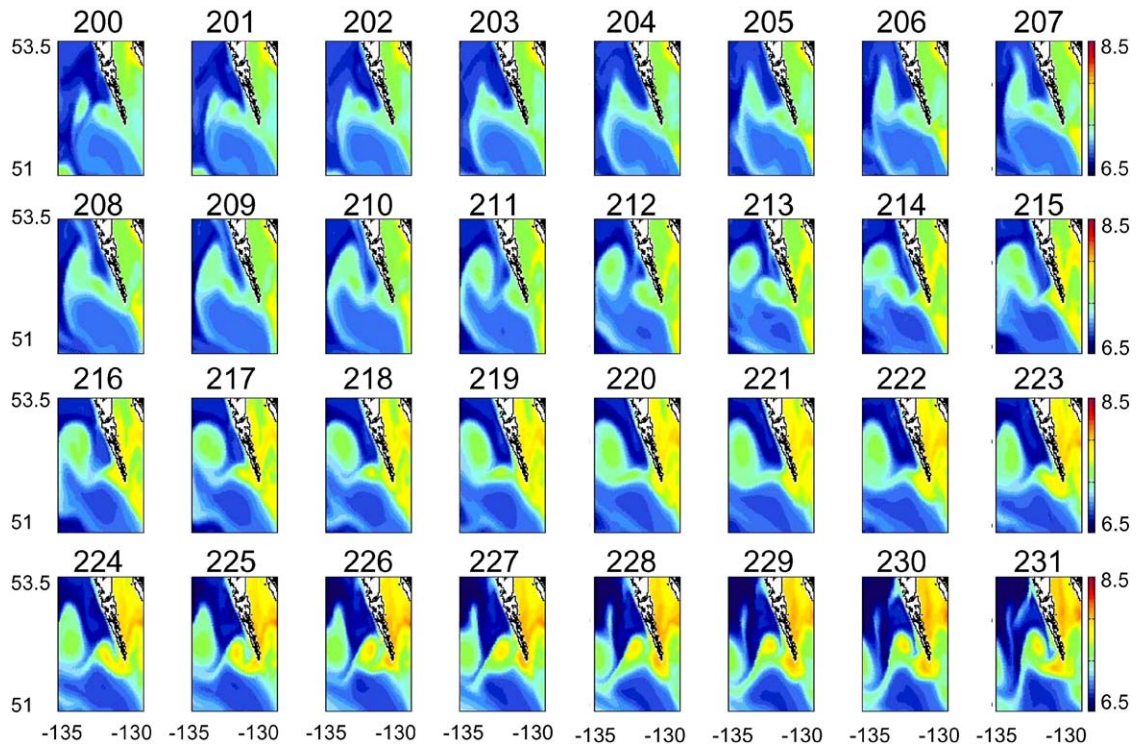


Fig. 6. Same time sequences (5-day interval) as in Fig. 5 but for model SST ($^{\circ}\text{C}$) arising from constant January winds and surface heat fluxes (experiment RUN_JAN).

shed from the cape. And the approximate size of our eddies at detachment is approximately 40 km, consistent with the Crawford et al. (2002) estimate based on CW00 formulae, and also consistent with satellite imagery for the Haida 1998a Eddy. In the case of the larger Haida Eddies, the core of the vortex, located further offshore, is intensified by the merging of several smaller anticyclonic eddies detaching from the cape and carrying patches of buoyant waters. A vertical section (Fig. 9) of the temperature composite anomalies along the path of the migrating smaller eddies (transect A2 in Fig. 8) during a more mature stage of the stronger offshore Haida Eddy, clearly shows the lens of mixed-layer warmer water spreading offshore from the cape. This anomaly is shallow close to the cape where the warm-buoyant patches are generated and extends deeper (to about 1000 m) offshore where the eddy has developed.

The importance of baroclinicity was also verified with an additional barotropic model simula-

tion where both T and S were set to constants over the entire model domain (experiment RUN_JAN_NO_BAR in Table 2). Consistent with Hannah et al. (1991), the model animation for this experiment shows that in the absence of horizontal and vertical density gradients no eddies are generated at the cape. The SSH mean for this simulation (Fig. 10C) does not show the path of the migrating eddies around Cape St. James and the flow follows the depth contours (a map of the bathymetry is shown in Fig. 10D for comparison). Sensitivity experiments to different strengths in cross-shore temperature gradient also were carried out. In general, they show that stronger cross-shore temperature gradients lead to more vigorous large eddies.

In summary, these model findings imply that Haida Eddies are baroclinic in nature and are generated by the advection of buoyant water masses flowing from Hecate Strait (and also from the southeast) around Cape St. James. These

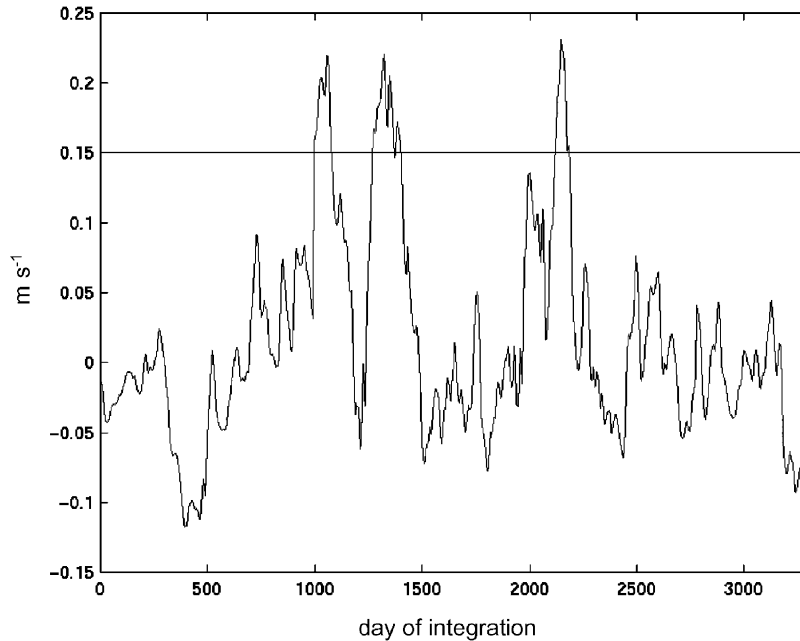


Fig. 7. Time series of model mean velocity normal to transect A1 (Fig. 3) from the simulation with constant January wind forcing (experiment RUN_JAN). Positive values are westward. Composite averaging of events above 0.15 m s^{-1} line are discussed in text and shown in Fig. 8.

plumes of buoyant flow intensify and sustain anticyclonic circulation immediately to the northwest of the cape and are therefore seen as anticyclonic eddies in the SSH field. When the flow is stronger, several of these eddies can merge to generate a larger eddy to the northwest. As will be shown later, stronger flow implies that the time for eddy formation is much shorter than the time over which the eddy drifts or is advected away from the generation location. Therefore, the Haida Eddy has more time to increase in size as more smaller eddies merge into it. We also find that the primary generation mechanism does not require the existence of an instability process, although instability processes (e.g., baroclinic instability) can affect the mean conditions under which they are formed. This was also noted by CW00.

5. The eddy shedding mechanism

The shedding of eddies in CW00 was found to occur when the timescale for eddy formation from

a buoyant current flowing around the cape was small compared to the timescale at which the eddies drifted away from the cape. In their experiments, sloping bathymetry in the deep ocean was used to simulate the planetary β effect and this slope sets the timescale of the drift. Conservation of potential vorticity associated with vortex stretching over sloping topography requires the eddies to drift along depth contours, with the deeper waters to the left. In the case of the Haida Eddy, this drift (Fig. 10D shows the bathymetry) should result in eddies moving northward along the west coast of the Queen Charlotte Islands. In addition to the topographic drift (i.e. topographic Rossby waves), Haida Eddies should also feel a drift due to the planetary β effect (Cushman-Roisin, 1994), which should cause them to move to the west. The combination of these two mechanisms should result in a northwest drift, and this direction is evident in the mean pathway of the eddies (Fig. 10A). We also note that Haida Eddies can be strongly affected by ambient currents that could intensify either the westward or the northward drifts.

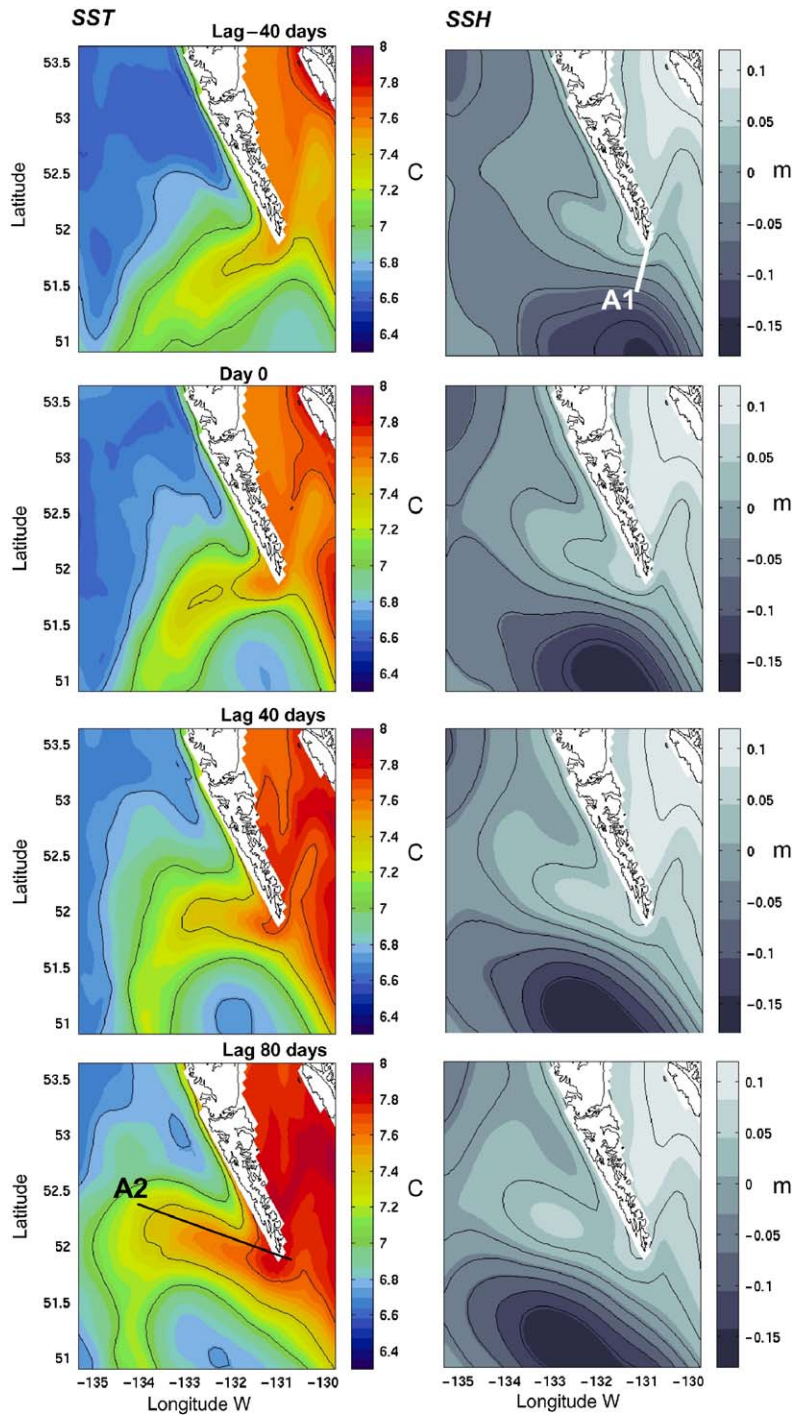


Fig. 8. Composite maps for SST and SSH for the eddy generation sequence in experiment RUN_JAN. See text for details on the averaging criteria.

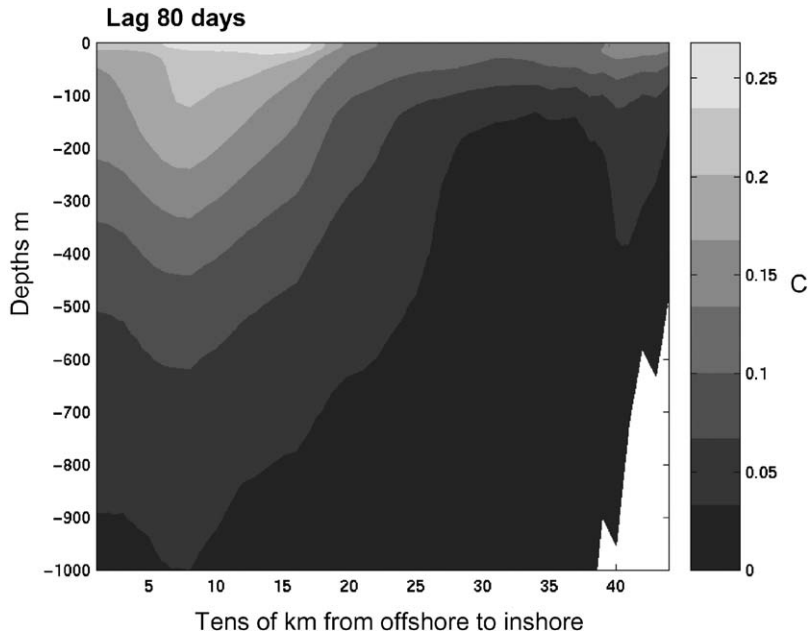


Fig. 9. Vertical section of composite temperature anomalies and bottom topography (white) for the upper 1000m along transect A2 for the 80-day lag panel of Fig. 8.

To isolate and further understand the effects of sloping topography versus meridional changes in planetary vorticity, we performed two experiments. The first experiment (case RUN_JAN_NO_BETA) retained the effect of sloping topography but had no meridional changes in planetary vorticity; i.e. no β effect ($\beta = 0$). The second experiment had flat topography but retained the effects of planetary β (case RUN_JAN_FLAT_H_BOUND). In the configuration of this second experiment, we also added an artificial coastline in northern Hecate Strait to preserve the mean southward flow past the east side of the cape (Fig. 10F). This flow is a necessary condition for the eddy generation. The need for this requirement is clearly seen by comparing the mean SSH for simulations with and without the additional coastline (compare Fig. 10F with Fig. 10E).

The long-term means for these two experiments are shown in Fig. 10B and F. Both experiments show a mean flow around the cape and to the north along the west coast of the Queen Charlotte Islands. In RUN_JAN_NO_BETA, the topographic constraint keeps the flow closer to the

coast and is stronger while in RUN_JAN_FLAT_H_BOUND the flow extends further to the west after it goes around the cape. Neither of these experiments shows clear signs of the same westward eddy propagation that was evident in the integration where both the effects of topography and β were retained (case RUN_JAN Fig. 10A). To better visualize the patterns of SSH associated with the larger eddies, we construct a composite of the eddy generation sequence for both these model simulations (Fig. 11) using the same criteria described before in Section 4 (for experiment RUN_JAN Fig. 8). A discussion of the sequence is provided below.

5.1. No β case

For the case with no β effect (case RUN_JAN_NO_BETA Fig. 11) the eddies are generated on the west side of the cape and then drift northward along the west coast of the Queen Charlotte Islands following the topographic contours. The drift is due to both the sloping topography and advection by the mean currents that are flowing in

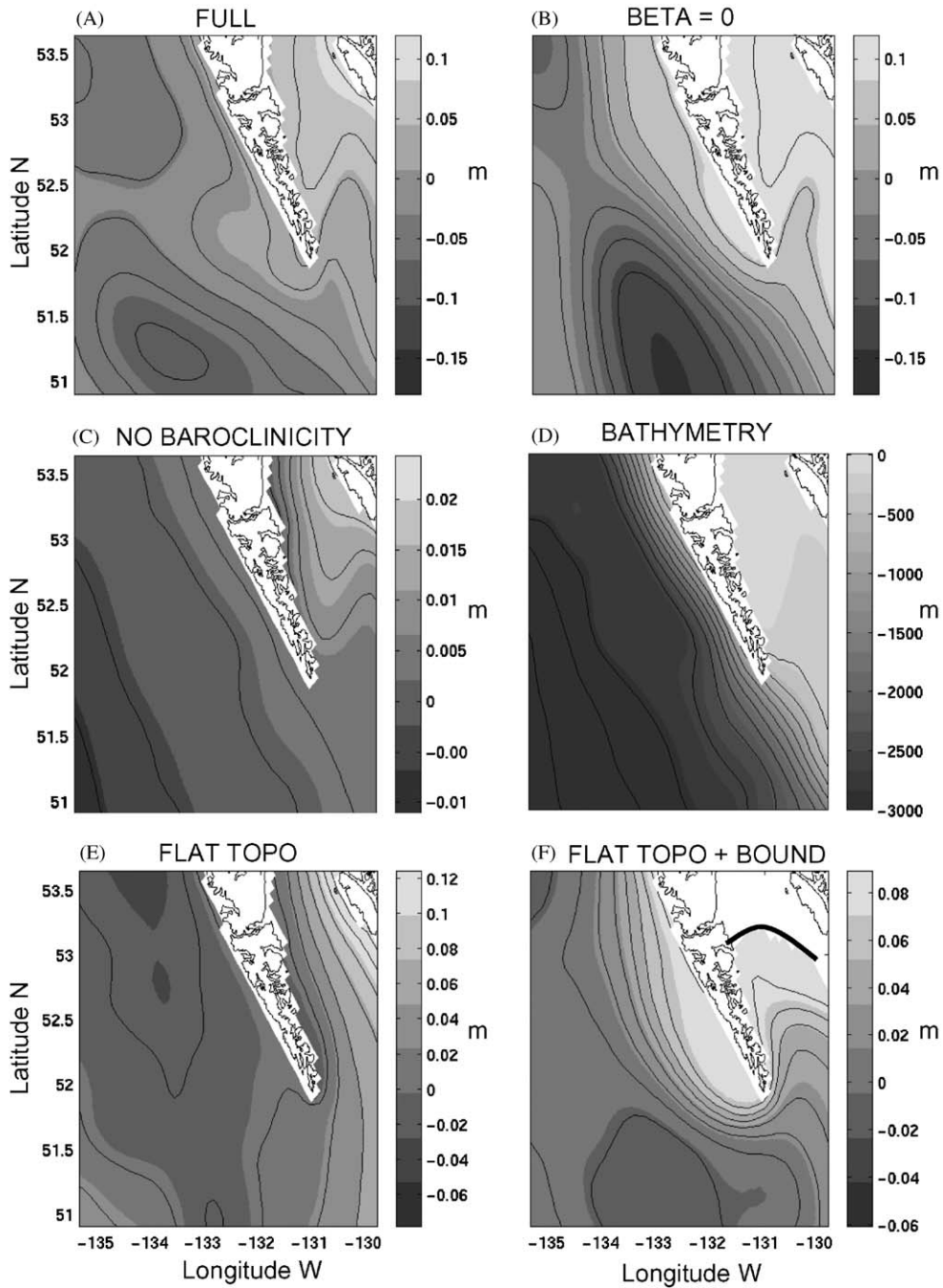


Fig. 10. Mean model SSH mean for different experiments: (A) RUN_JAN; (B) RUN_JAN_NO_BETA; (C) RUN_JAN_NO_BAR; (E) RUN_JAN_FLAT_H; and (F) RUN_JAN_FLAT_H_BOUND. Panel (D) shows the non-flat bathymetry. The solid line in (F) denotes the artificial coast.

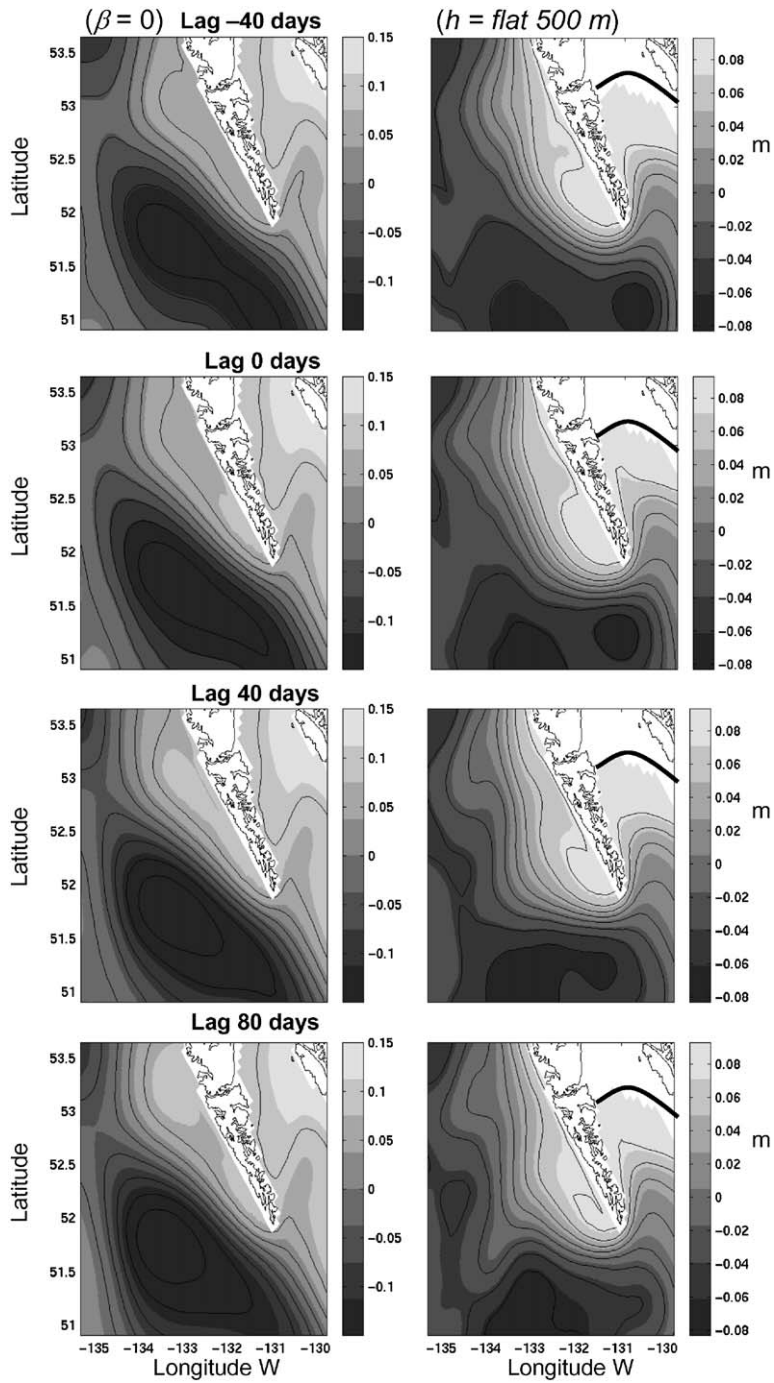


Fig. 11. Composite maps of SSH for the eddy generation sequence in experiment RUN_JAN_NO_BETA ($\beta = 0$) (left column) and RUN_JAN_FLAT_BOUND (flat topography) (right column). See text for details on the averaging criteria.

the same northward direction. A similar behaviour also was found in CW00 when they changed the orientation of the cape to be along the drift direction. An animation of this model run shows that bigger eddies are the result of several mergers of smaller eddies; a result previously seen for the full case (experiment RUN_JAN). Eventually, some of the big eddies interact with offshore currents and are removed from the shelf after generating eddy dipole structures (Fig. 11). This is more clearly seen if we repeat the same simulation with the seasonal cycle of the winds included (an animation of this case is also available at <http://www-sci.pac.dfo-mpo.gc.ca/dsr2/>). The generation and existence of the stronger eddies suggest that for this case, the formation timescale is short compared to the time of the drift, which occurs along the depth contour.

5.2. Flat bottom case

In the generation sequence for the case with flat topography (case RUN_JAN_FLAT_BOUND Fig. 11), we again find an intensification of positive SSH around and to the west of the cape (lag -40 and 0 in Fig. 11). However, as time progresses, we do not find any sign of detachment and drift of large eddies westward, as one would expect from the β effect. Instead we find that the eddy intensifies in place and the northward flowing currents around the offshore perimeter of the eddy and along the west coast of the Queen Charlotte Islands start meandering (lag 40 and 80). Small eddies detach from these meanders and are then seen to migrate to the west. Successive time snapshots of one particular event (Fig. 12) show the detachment of smaller eddies from meanders in the flow around a large eddy resident at the cape. The time interval between the snapshots is 10 days. At day 0 we find two meanders labelled M1 and M2 in Fig. 12. As we progress to day 20, meander M1 is starting to detach and migrate to the west while at day 30, M1 is fully detached as an eddy and M2 is beginning to detach and merge with M1. These smaller detached eddies never reach the size and strength of the Haida Eddies as described in the previous sections, and their generation mechanism is clearly associated with instabilities in

the meandering currents around the standing eddy at the cape. The existence of a standing eddy at the cape was also reported in CW00 (Section 8) when their bottom slope was chosen sufficiently small to represent only the planetary β effect. In this case, a standing anticyclonic vortex developed but did not detach or drift from the cape, though some fluid within the vortex leaked and drifted westward.

In general, the flat bottom experiment seems to have produced a baroclinically more unstable circulation off Cape St. James. In other words, bottom topography seems have a stabilizing effect on the local circulation; a result that is consistent with quasi-geostrophic turbulence and other modelling studies (Marchesiello et al., 2003; Barth, 1994; CW00).

In order to test the effects of increasing the speed of the flows past the cape on the time of eddy formation and detachment, we performed an additional experiment in which the amplitude of the wind stress was increased by a factor of three. Unfortunately, this experiment did not lead to a significant increase in flow around the cape and this sensitivity analysis is left for future studies. Another sensitivity experiment for the flat bottom case was carried out with free-slip lateral boundary conditions, instead of no-slip. The results did not change significantly although we noticed that in the free-slip case, the meandering of the currents on the outer perimeter of the standing eddies was reduced on average.

5.3. Sensitivity to advection

Though not discussed by Cummins and Oey (1997), previous simulations of baroclinic tidal flows around Cape St. James with the Princeton Ocean Model and a 5-km resolution were unable to capture the generation of the anticyclonic eddies (Patrick Cummins, pers. comm.) that were observed by Thomson and Wilson (1987). Motivated by the suggestion that this might have been due to the second-order advection scheme used in these simulations, we performed an additional integration for experiment RUN_JAN using a second-order centred advection scheme, instead of the third-order upstream bias scheme. This sensitivity experiment is denoted as RUN_JAN_ADV2 in

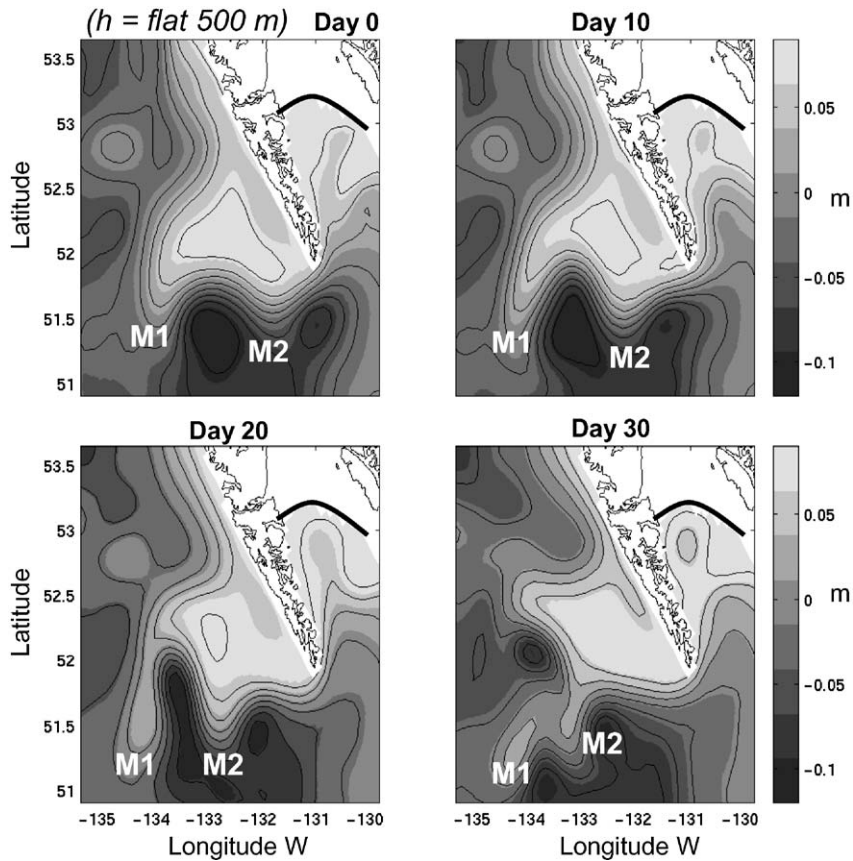


Fig. 12. Model SSH time sequence extracted from the experiment with flat bottom topography (case RUN_JAN_FLAT_BOUND). Solid line denotes the artificial coastline that ensures counterclockwise flow around Hecate Strait. Day 0 denotes the beginning of the extracted sequence, not of the model integration. M1 and M2 denote meanders discussed in the text.

Table 2. Comparing the SSH animation for this simulation with RUN_JAN (<http://www-sci-pac.dfo-mpo.gc.ca/dsr2/>) reveals that although the former case still has a tendency to generate eddy-like patterns at the cape, the anticyclonic recirculation associated with these patches of buoyant flow fails to turn into coherent anticyclonic eddies and is quickly dissipated. That is, strong Haida Eddies are not formed. Consequently, a lower-order numerical approximation for the advective terms does make a noticeable difference. For the horizontal resolution used in these simulations, it seems that third-order advection is required for a reasonably accurate representation of the strong Haida Eddies observed by satellite altimeters and in situ measurements.

6. Summary and discussion

Numerical simulations of the annual cycle and simple process studies have demonstrated that Haida Eddies are regularly generated off Cape St. James in the winter. Model sensitivity studies to different forcing showed that Haida Eddies are baroclinic in nature, as previously observed by Crawford (2002), and are generated by the merging of several smaller eddies generated on the northwest side of Cape St. James. In the model, similar to the observations, the vertical extent of the larger eddies is roughly 1000 m and a typical generation and shedding cycle is roughly 3 months. Consistent with the findings of CW00 and the suggestions in CCFG02, mean advection of

warmer fresher water around the cape from Hecate Strait generates plumes of buoyant flow, which intensify and sustain small patches of anticyclonic circulation immediately to the northwest of the cape. When the flow is strong, several of these smaller eddies can merge to generate a larger feature, the Haida Eddy. Cross-shore density gradients between the waters in Hecate Strait and those offshore and to the north along the west coast of the Queen Charlotte Islands also can affect the strength of the eddies. Because of this generation mechanism, fully developed offshore eddies are characterized by water properties typical of inshore locations.

In contrast to the suggestions given in Melsom et al. (1999) and Murray et al. (2001), our findings imply that the primary generation mechanism does not require an instability process (e.g., baroclinic instability), although such processes can affect the conditions under which they are formed. We suspect the main reason that the Melsom et al. (1999) and Murray et al. (2001) studies did not come to the same conclusion was that their grids omitted Hecate Strait and Queen Charlotte Sound and thus did not have strong flows past a promontory. This is not to say that baroclinic instability is not a generation mechanism for other eddies generated along the British Columbia and Alaska shelves. In fact, the satellite images and arguments presented in Thomson and Gower (1998) suggest that baroclinic instability is a relevant process, that in some instances may even act in conjunction with the different Haida Eddy formation mechanism described here.

An accurate representation of bathymetry also was found to be important for the generation and shedding processes. Dynamical constraints associated with the depth contours are required to sustain the mean currents around the cape and to limit the area of offshore spread of the buoyant water from Hecate Strait. The dynamical response to such a limitation is the generation of smaller eddies, which can either drift away from the cape as standalone eddies or merge into a bigger Haida Eddy offshore, particularly when the rate at which they are formed is higher due to stronger currents. In the absence of topography (e.g., a flat bottom), the buoyant flow from Hecate Strait can spread

further offshore and a large standing eddy can develop at the cape without ever detaching. However, smaller eddies can detach from the meanders along the offshore perimeter of the standing eddies and drift to the west. The standalone eddy generation process is the same as for the Haida Eddy, while the generation of smaller eddies from the meanders is likely associated with instability processes.

In the model, Haida Eddies also can be generated by neglecting the effect of meridional changes in planetary vorticity ($\beta = 0$). These eddies arise from the merger of smaller eddies originating at the cape and then drift along depth contours as they intensify along the west coast of the Queen Charlotte Islands. Eventually, they give rise to dipole structures as they are removed from the shelf region through interactions with the offshore current.

Whitney and Robert (2002) (and other papers in this issue) suggest that Haida Eddies play a significant role in transferring nutrients and larvae from Hecate Strait to the ambient ocean. A major challenge for future modelling studies will be to predict the generation and evolution of these eddies so that better estimates of productivity and recruitment can be provided to ecosystem managers.

Acknowledgements

Funding for EDL was provided by NOAA (NA17RJ1231 through CIFAR) and NASA (NAG5-9788). MGGF and WRC were partially funded by the Hecate Strait Ecosystem and Haida Eddy Strategic Science Funds of Fisheries and Oceans Canada. The views expressed herein are those of the author(s) and do not necessarily reflect the views of NOAA or any of its sub-agencies. Supercomputing resources were provided by NASA. The NCEP re-analysis data were provided by the NOAA-CIRES Climate Diagnostics Center, Boulder, CO, USA, from their Web site at <http://www.cdc.noaa.gov/>. We thank Josef Cherniawsky for TOPEX/POSEIDON altimetry, and the Canadian Hydrographic Service and NOAA (http://co-ops.nos.noaa.gov/data_res.html) for tide gauge data.

References

- Barth, J.A., 1994. Short-wavelength instabilities on coastal jets and fronts. *Journal of Geophysical Research—Oceans* 99 (C8), 16095–16115.
- Batten, S., Crawford, W.R., 2005. The influence of coastal origin eddies on oceanic plankton distributions in the eastern Gulf of Alaska. *Deep-Sea Research II* [doi:10.1016/j.dsr2.2005.02.009].
- Bretherton, F.P., Davis, R.E., Fandry, C.B., 1976. Technique for objective analysis and design of oceanographic experiments applied to MODE-73. *Deep-Sea Research* 23 (7), 559–582.
- Cenedese, C., Whitehead, J.A., 2000. Eddy shedding from a boundary current around a cape over a sloping bottom. *Journal of Physical Oceanography* 30 (7), 1514–1531.
- Cherniawsky, J.Y., Crawford, W.R., 1996. Comparison between weather buoy and comprehensive ocean-atmosphere data set wind data for the west coast of Canada. *Journal of Geophysical Research—Oceans* 101 (C8), 18377–18389.
- Cherniawsky, J.Y., Foreman, M.G.G., Crawford, W.R., Henry, R.F., 2001. Ocean tides from TOPEX/Poseidon sea level data. *Journal of Atmospheric and Oceanic Technology* 18 (4), 649–664.
- Crawford, W.R., 2002. Physical characteristics of Haida Eddies. *Journal of Oceanography* 58 (5), 703–713.
- Crawford, W.R., Cherniawsky, J.Y., Foreman, M.G.G., Gower, J.F.R., 2002. Formation of the Haida-1998 oceanic eddy. *Journal of Geophysical Research* 107 (C7), 3069.
- Crawford, W.R., Brickley, P.J., Peterson, T.D., Thomas, A.C., 2003. “Impact of Haida Eddies on chlorophyll distribution in the eastern Gulf of Alaska.” (this issue) [doi:10.1016/j.dsr2.2005.02.011].
- Cummins, P.F., Oey, L.Y., 1997. Simulation of barotropic and baroclinic tides off northern British Columbia. *Journal of Physical Oceanography* 27 (5), 762–781.
- Cushman-Roisin, B., 1994. *Introduction to Geophysical Fluid Dynamics*. Prentice-Hall, Englewood Cliffs, NJ, p. 320.
- Di Lorenzo, E., 2003. Seasonal dynamics of the surface circulation in the Southern California Current System. *Deep-Sea Research II* 50 (14–16), 2371–2388.
- Faucher, M., Burrows, W.R., Pandolfo, L., 1999. Empirical–statistical reconstruction of surface marine winds along the western coast of Canada. *Climate Research* 11 (3), 173–190.
- Foreman, M.G.G., Crawford, W.R., Cherniawsky, J.Y., Gower, J.F.R., Cuypers, L., Ballantyne, V.A., 1998. Tidal correction of TOPEX/POSEIDON altimetry for seasonal sea surface elevation and current determination off the Pacific coast of Canada. *Journal of Geophysical Research—Oceans* 103 (C12), 27979–27998.
- Haidvogel, D.B., Arango, H.G., Hedstrom, K., Beckmann, A., Malanotte-Rizzoli, P., Shchepetkin, A.F., 2000. Model evaluation experiments in the North Atlantic Basin: simulations in nonlinear terrain-following coordinates. *Dynamics of Atmospheres and Oceans* 32 (3–4), 239–281.
- Hannah, C.G., LeBlond, P.H., Crawford, W.R., Budgell, W.P., 1991. Wind-driven depth-averaged circulation in Queen Charlotte Sound and Hecate Strait. *Atmosphere–Ocean* 29, 712–736.
- Hurlburt, H.E., Wallcraft, A.J., Schmitz, W.J., Hogan, P.J., Metzger, E.J., 1996. Dynamics of the Kuroshio/Oyashio current system using eddy-resolving models of the North Pacific Ocean. *Journal of Geophysical Research—Oceans* 101 (C1), 941–976.
- Koblinsky, C.J., Ray, R., Beckley, B.D., Wang, Y.-M., Tsaoussi, L., Brenner, A., Williamson, R., 1999. NASA Ocean Altimeter Pathfinder Project Report 1: Data Processing Handbook. NASA/TM-1998-208605.
- Johnson, W.K., Miller, L.A., Sutherland, N.E., Wong, C.S., 2005. Iron transport by mesoscale Haida Eddies in the Gulf of Alaska. *Deep-Sea Research II* [doi:10.1016/j.dsr2.2004.08.017].
- Large, W.G., McWilliams, J.C., Doney, S.C., 1994. Oceanic vertical mixing—a review and a model with a nonlocal boundary layer parameterization. *Reviews of Geophysics* 32 (4), 363–403.
- Levitus, S., Burgett, R., Boyer, T.P., 1994. *World Ocean Atlas 1994*. NOAA Atlas NESDIS 4, US Government Printing Office, Washington, DC, pp. 3–4.
- Mackas, D.L., Galbraith, M., 2002. Zooplankton community composition along the inner portion of Line P during the 1997–1998 El Niño event. *PROGRESS IN OCEANOGRAPHY* 54 (1–4), 423–437.
- Marchesiello, P., McWilliams, J.C., Shchepetkin, A., 2001a. Equilibrium structure and dynamics of the California Current System. *Journal of Physical Oceanography* 33 (4), 753–783.
- Marchesiello, P., McWilliams, J.C., Shchepetkin, A., 2001b. Open boundary conditions for long-term integration of regional oceanic models. *Ocean Modelling* 3, 1–20.
- Marchesiello, P., McWilliams, J.C., Shchepetkin, A., 2003. Equilibrium structure and dynamics of the California Current System. *JOURNAL OF PHYSICAL OCEANOGRAPHY* 33 (4), 753–783.
- Melson, A., Meyers, S.D., Hurlburt, H.E., Metzger, E.J., O’Brien, J.J., 1999. ENSO effects on Gulf of Alaska eddies. *Earth Interactions* 3 (1) (available at: <http://EarthInteractions.org>).
- Murray, C.P., Morey, S.L., O’Brien, J.J., 2001. Interannual variability of upper ocean vorticity balances in the Gulf of Alaska. *Journal of Geophysical Research—Oceans* 106 (C3), 4479–4491.
- Nof, D., Pichevin, T., Sprintall, J., 2002. “Teddies” and the origin of the Leeuwin Current. *JOURNAL OF PHYSICAL OCEANOGRAPHY* 32 (9), 2571–2588.
- Shchepetkin, A., McWilliams, J.C., 1998. Quasi-monotone advection schemes based on explicit locally adaptive dissipation. *Monthly Weather Review* (126), 1541–1580.
- Shchepetkin, A.F., McWilliams, J.C., 2003. A method for computing horizontal pressure-gradient force in an oceanic model with a non-aligned vertical coordinate. *Journal of Geophysical Research—Oceans* 108 (C3).

- She, J., Klinck, J.M., 2000. Flow near submarine canyons driven by constant winds. *Journal of Geophysical Research—Oceans* 105 (C12), 28671–28694.
- Smith, W.H.F., Sandwell, D.T., 1997. Global sea floor topography from satellite altimetry and ship depth soundings. *Science* 277 (5334), 1956–1962.
- Song, Y., Haidvogel, D., 1994. A semi-implicit ocean circulation model using a generalized topography-following coordinate system. *Journal of Computational Physics* 115 (1), 228–244.
- Tabata, S., 1982. The anticyclonic, baroclinic eddy off Sitka, Alaska, in the northeast Pacific Ocean. *Journal of Physical Oceanography* 12 (11), 1260–1282.
- Thomson, R.E., Gower, J.F.R., 1998. A basin-scale oceanic instability event in the Gulf of Alaska. *Journal of Geophysical Research—Oceans* 103 (C2), 3033–3040.
- Thomson, R.E., Wilson, R.E., 1987. Coastal countercurrent and mesoscale eddy formation by tidal rectification near an oceanic cape. *Journal of Physical Oceanography* 17 (11), 2096–2126.
- Whitney, F., Robert, M., 2002. Structure of Haida Eddies and their transport of nutrient from coastal margins into the NE Pacific Ocean. *Journal of Oceanography* 58 (5), 715–723.

Further reading

- Crawford, W.R., Brickley, P.J., Peterson, T.D., Thomas, A.C., this issue. Impact of Haida Eddies on chlorophyll distribution in the eastern Gulf of Alaska. *Deep-Sea Research II* [doi:10.1016/j.dsr2.2005.02.011]
- Kudela, R.M., Chavez, F.P., 2002. Multi-platform remote sensing of new production in central California during the 1997–1998 El Niño. *Progress in Oceanography* 54 (1–4), 233–249.
- Strub, P.T., James, C., 2002. Altimeter-derived surface circulation in the large-scale NE Pacific Gyres. Part 2: 1997–1998 El Niño anomalies. *Progress in Oceanography* 53 (2–4), 185–214.